Modified method of spectral analysis of the reflection signal for damage detection systems in power lines

Kostyantyn Horiaschenko[1], Victor Stetcuk[1]
[1]Khmelnitsky national university, Khmelnitsky, Ukraine
Corresponding autor: Kostyantyn Horiaschenko
E-mail: kostyakst@ukr.net, sv_rt@i.ua

Abstract. The work is devoted to the aspects of using phase methods for measuring distances to faults in a power line. The existing phase methods are shown and discussed. It is established that spectral leakage is one of the problems of spectral analysis. An algorithm for spectral analysis based on a change in the width of the analysis window is proposed. It is shown that the proposed method provides an increase in the accuracy of determining the amplitudes of the total signal components.

Keywords: power line, phase angle shift, spectral analysis, spectral leakage.

1. Introductions

1.1. The problem of measuring of parameters of power lines

Controlling of power lines state is a well-known problem. Usually measuring of parameters of such lines requires two categories of actions [13]:

1) The first category is a global analysis. Global analysis consists in determination of the state of the whole power line. As a result, we have information about state of whole line. In compare with previously measured data, detailed measuring can be required.

2) The second category is a local analysis. Analysis consists in measuring of parameters from point to point. Many methods used to do such measuring. However, each of them has advantages and disadvantages.

The presented categories connected to each other but they does not interchangeable. The methods in the first category put on an aim verification of readiness to work or accordance of the already on-the-road system to the further use. Therefore, we have information about state of all power line. The methods in the second category used not only with the aim of measuring of parameters of power lines. A principal difference is ability for determination of current state of each part of power line. As a result, we can control local damages at any distance in line.

Measuring of parameters of the power line or system of power lines is a difficult process which require the use of one or a few simultaneously technologies.

A lot modern methodologies used for implementation of measuring [3, 8, 13]:

1. Time Domain Reflectometry, TDR.

2. Partial Discharge, PD (working frequencies varies from 50/60 Hz down-to 0,02 Hz (VLF)).

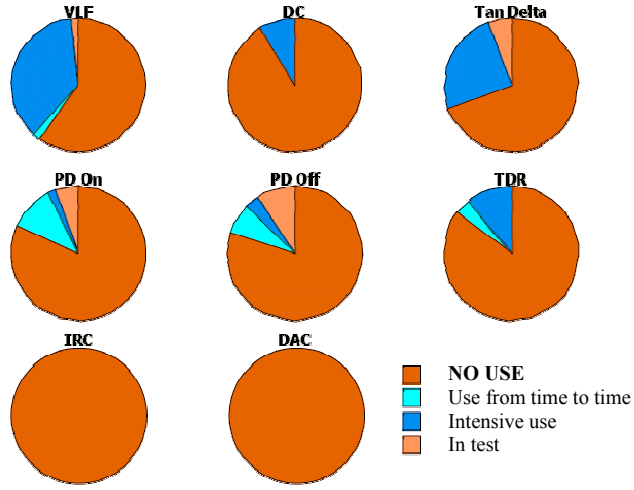

Fig. 1. The methods of measuring: VLF - very low frequency; DC – direct current; Tan Delta (tgδ) –measuring of dielectric losses; PD On and PD – partial discharge methods, TDR – time domain reflectometry; IRC - Isothermal Relaxation Current; DAC - Damped AC

3. tg δ (tan δ), analysis of the dielectric penetrating on different frequencies.
4. Measuring of recovery Voltage.
5. DC Leakage Current.
6. Application of combinations of methods.

Many from these measuring methods already used in measuring devices, others are not yet accepted [11]. The use of various methods of measuring in power lines in the USA [13] are shown on fig. 1.

For practical use only VLF, tg δ and TDR accepted. Other methods are on the stage of research or do not have commercial use. We have two fundamental groups:

а) The destructive measuring methods based on use of over-voltages. Such methods not only detect defects, they speed-up destruction of power lines.

б) The non-destructive measuring methods based on use of low and nominal voltages. Those methods can be used without interrupting normal work of power lines.

1.2. Known phase measuring methods for distance measuring

1.2.1. Classic phase measuring method

Phase measuring methods based on measuring of phase shift [20, 21, 22] between applied test signal $\omega_0 = U_{m1}\cos\varphi_1$ and returned signal from reflection:

$$\omega_{01} = U_{m1}\cos\left(\Omega_m t + \varphi_{01}\right), \tag{1}$$

where U_{m1} – an amplitude of test signal;

Ω_m – a frequency of scale frequency, in simplest case $\Omega_m = \omega_0$;

φ_{01} – a phase angle shift on frequency ω_0 for the some object in line.

The returned signal looks like :

$$s_2(t) = U_{m2}\cos\varphi_2 = U_{m2}\cos\left(\Omega_m\left(t - t_R\right) + \varphi_{01} + \varphi_{ap} + \varphi_{\text{ret}}\right), \tag{2}$$

where U_{m2} - amplitude of returned signal;

φ_{01} - an initial angle;

φ_{ap} - a angle shift in the apparatus;

φ_{ret} - a phase angle shift at the reflection.

Distance to reflection in air determined as [20, 21, 23]:

$$R = \frac{c\left(\varphi_\Delta + \varphi_{ap} + \varphi_{\text{ret}}\right)}{2\Omega_m} \text{ or } R = \frac{c\left(\varphi_\Delta + \varphi_{ap} + \varphi_{ret}\right)}{2\omega_0}, \tag{3}$$

where c –speed of signal in air.

For a physical environment with speed of distribution υ distance will be determined as:

$$R = \frac{\upsilon\left(\varphi_\Delta + \varphi_{ap} + \varphi_{ret}\right)}{2\omega_0}. \tag{4}$$

A value of phase angle shift φ_{ap} can be eliminated by calibration. The phase angle shift at the reflection of signal φ_{ret} strongly influence with result – distance. That is why for measuring distance by phase angle shift method value of φ_{ret} is only ±180° (fig. 2).

Use of classical phase measuring method based on the following principles in case of two or more reflections in any electrical line [19]:

- all signals pass through environments without fading;
- speeds of wave distribution in all environments are identical;
- a signal is reflected in accordance with to the reflection coefficient of this object;
- size of damage as small as possible, a zero-size of damage used as a rule;

- signals passes power line pass without distortions.

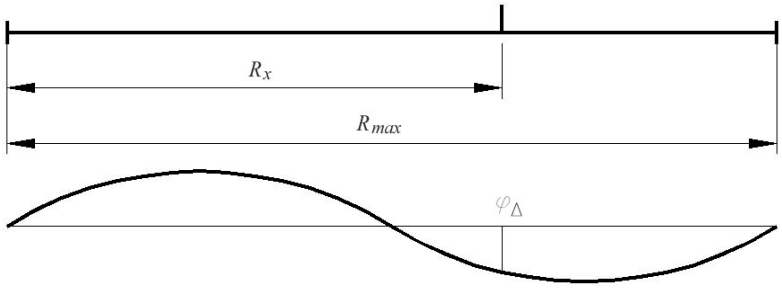

Fig. 2. Phase angle shift method

Simple case of two objects is shown on fig. 3. Objects are located at distances l_1 and l_2 from the start of line. Accord to shown principles, a signal from the first object will be reflected with a phase angle shift φ_1. A **phase angle shift** can be expected after a formula:

$$\varphi_1 = 2 \cdot 2\pi \frac{l_1}{L_{\max}}. \tag{5}$$

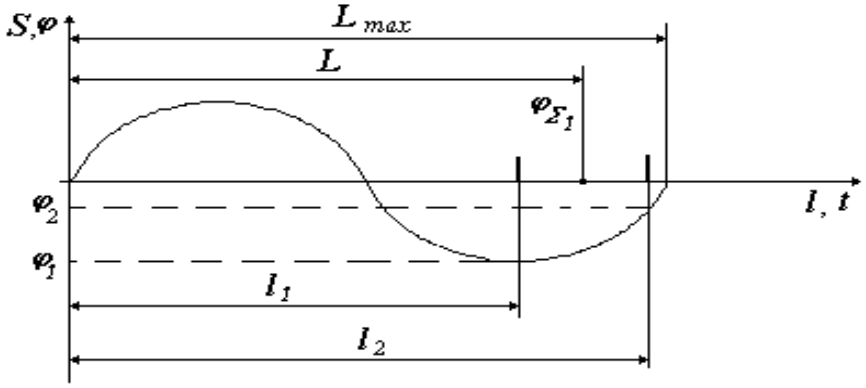

Fig. 3 Phase angle sift in case of existence of two objects

For the second object a **phase angle shift** φ_2 will be:

$$\varphi_2 = 2 \cdot 2\pi \frac{l_2}{L_{\max}}. \tag{6}$$

Amplitudes of signals from every object depend on reflection coefficients Γ_1, Γ_2 and amplitudes of input signal a. Thus, we have:

$$a_1 = \Gamma_1 a\ ,\ a_2 = \Gamma_2 a\ . \tag{7}$$

All signals are harmonious with one frequency and different phase changes. Thus:

$$s_{refl\,\Sigma}(t) = a_1 \cos(\omega t + \varphi_1) + a_2 \cos(\omega t + \varphi_2). \tag{8}$$

In this case, from (10) with use of (4) we will receive signal like $s_{refl\Sigma}(t) = A_\Sigma \cos(\omega t + \varphi_\Sigma)$ – signal from imaginary one object. And this object not at distance l_1 or l_2. This expression shows the most problem of classic phase distance measuring method – no possibility to separate objects in the process of measuring.

Other problem we have is a case of vagueness of distance measuring when a wave-length λ less than length of line L. Distance:

$$l = \lambda(2\pi \cdot n + \varphi)/2\pi ,$$

where n is integer from 0 to $\lfloor L/\lambda \rfloor$.

For the measuring with higher accuracy used so-called multiscale method [17, 18]. This method based on forming of set of frequencies from the most low frequency, wave-length of which will be greater than length of line which is tested.

Advantages of that method:

- high exactness of determination of change of phases allows to get high exactness of distance-finding to the damage;
- using of low frequencies allows to simplify construction of measuring device and diminishes a sensitivity to the external factors;
- measuring phase angle shift is possibly during long time which improves overall accuracy.

1.3. Modern phase angle shift measuring methods and devices

With grow of electronic devices with large memories and high speeds new methods of distance measuring were developed. Those methods are based on use of sine wave signals and measuring of frequency of beating, as functions of distances [4, 9, 15]. Unlike TDR, new methods belong to frequency dimension reflectometry (FDR).

There are three types of frequency dimension reflectometry that use for measuring distances to damages. To such methods belong:

1) Frequency Modulated Continuous Wave (FMCW) [10, 5, 16];
2) Phase Detection Frequency Domain Reflectometry (PD-FDR) [10, 16];
3) Standing Wave Reflectometry (SWR).

Let consider shortly each of them.

1.3.1. Frequency Modulated Continuous Wave (FMCW)

FMCW change frequency of sine wave signal very quickly. As a result, frequency shift measured between test and reflection signals converted to a corresponding delay equivalent to distance to the object. However, this method did not find application in power lines through limitation on speed in which a signal can spread in a line. Insufficient accuracy in which the frequency shift can be determined [9] is also determined.

1.3.2. Phase Detection Frequency Domain Reflectometry (PD - FDR)

System of measuring of distance which is based on measuring of phase angle shift shown on fig. 4 [5, 6, 7], measures a phase angle shift between entrance and initial signals.

A voltage controlled generator (VCO) provides a sine wave signal which steps in a line through the signal divider with a separation weak by -10 dB signal of the so-called "copy" of test signal (first mixer), and returns back in a device through the second mixer.

A mixer mixes together two sine wave that gives a sum and difference of these two frequencies. After that, analogue signals transformed to digital ones for fast Fourier transformation. This is a first method

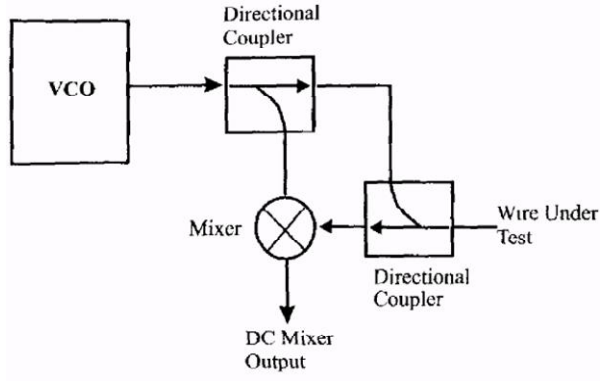

Fig. 4 Flow-chart of PD – FDR [7]

offered the use of accumulation of measuring information and treatment of them in a single informative block.

FFT of the accumulated signal give a peak signals. Places of peaks in spectrum of FFT will give distances to each of them. Distance can be found as [7]:

$$L = 2L_{\max}\left(\frac{Peak - Peak(0)}{N_{FFT} - 1}\right) = \frac{1}{2}\left(\frac{Peak - Peak(0)}{N_{FFT} - 1}\right)\left(\frac{N_F - 1}{f_2 - f_1}\right)\upsilon_p . \quad (9)$$

where $Peak$ – location of peak of delta function in FFT (integer value);

υ_p –speed of distribution in a cable (m/s);

f_1 –initial frequency of FDR (Hz)

f_2 –eventual frequency of FDR (Hz)

N_F –number of frequencies in FDR, usually unit from $Int\left(\frac{f_2 - f_1}{\Delta f}\right)$;

Δf –size of step of frequency for FDR (Hz);

$L_{\max}$ –maximal length, shown below;

N_{FFT} –number of points in FFT (integer value, on the whole 1024, 2048, 4096 or 8192).

The fundamental problem of PD-FDR is very high count of points for FFT, low separation ability of objects and large range of frequencies. The typical set of answers of different lengths (on the example of wire as M27500 - 24SE2S23, [7]) is shown on Fig. 5.

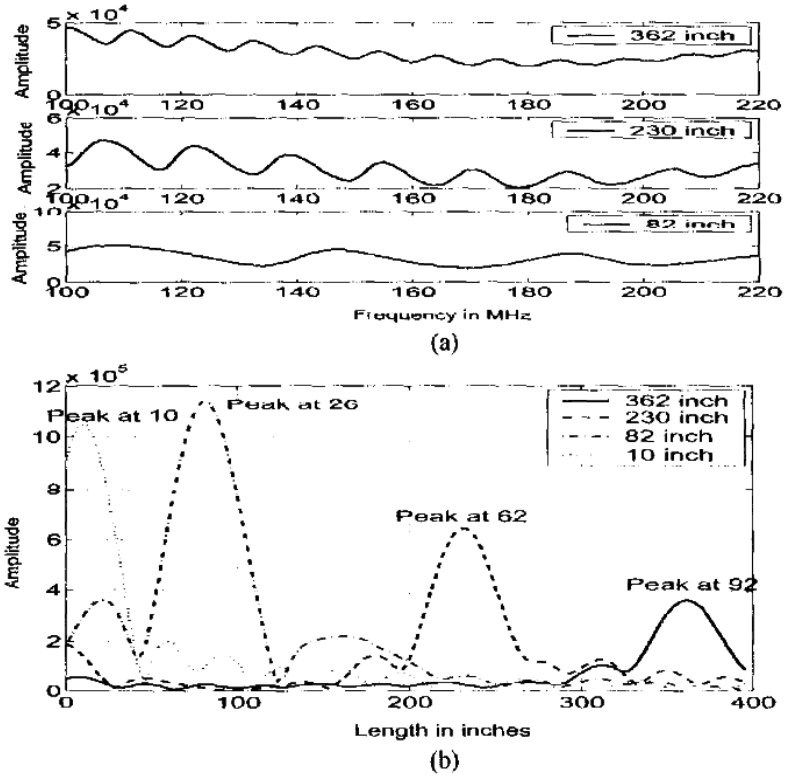

Fig. 5 Result of PD-FDR for the coaxial cable of RG-58 (50ohm):
a) result on the exit of mixer; b) result of FFT [7]

PD-FDR has lower cost and uses simpler electronic base in compare with TDR. Components for PD-FDR could be integrated in a single chip. In addition, PD-FDR is able to work with re-

reflections.

Like to the method of TDR of diminishing to distance to the object from the beginning of line requires minimisation of test signal frequency. But this is not possible to very low frequencies [2, 5, 14].

1.3.3. Standing Wave Reflectometry (SWR)

Standing Wave Reflectometry measure the size of standing wave, created by imposition of test and reflected signals from line. A sum of these signals is two sinewave signals (see (10)) which usually identical amplitude. However, the problem of SWR is a detection of signals with low level of reflection. Therefore, the method of SWR used in case of short circuit or break.

Advantages of SWF are exactness, similar to PD-FDR in case of short circuit or break, where test and reflected signals approximately the same size. The reflected wave will be partly less, depending on distance, but require frequencies in kHz for measure.

1.3.4. Mixed signal reflectometry (MSR)

Mixed signal reflectometry (Fig. 6) is similar to PD-FDR without direction couplers or to SWR, which measures the size of standing wave. Like PD-FDR, voltage controlled oscillator (VCO) provides a sine wave signal which steps above the given size of step. Combination of test and reflected signals passes through attenuator, which prevent the overload of mixer.

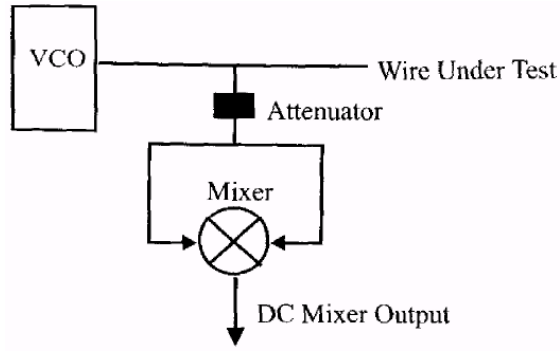

Fig. 6 Scheme diagram of MSR [7]

The method of MSR is more exact, than SWR for small reflections. However, this advantage does not have practical application, because it does not allow analysing very little anomalies. MSR is less expensive and less cost than PD-FDR. For the lines with interconnections, reflected signal of MSR includes reflections plus their sums and differences, which does the answer more difficult for a calculation than PD - FDR. MSR have the same limitation on the use on live wires identically to PD-FDR.

1.4. Phase method for measuring distances of simultaneous objects in power line

Classic phase measuring method based on determination of phase angle shift φ between test input signal and reflection of the known frequency f_s [20, 21, 23].

A vector diagram (fig. 7) serves for explanation of problem of phase methods. Diagram shows forming of summary signal $U_\Sigma \cos\varphi_\Sigma$ [19]. An analogical diagram can be created for 3-rd, 4-th or other amount of damages. A result is an signal of reflection with the corresponding summary phase angle shift φ_Σ.

Multiscale method of measuring of distances to the damages leading and optical to the flow line it is known from works of such scientists as Maevsky S.M., Bajenov V.H., Baturevich E.K. The multifrequency phase measuring method is used practically for measuring.

On Fig. 8 presented reflecting in the case of two objects with zero-size damages. Distances to the damages accordingly $l_1 = 1000$ м, $l_2 = 2000$ м. Amplitude of the first reflection has a level a 1,0 units (vector A), second is 0,5 units (vector B).

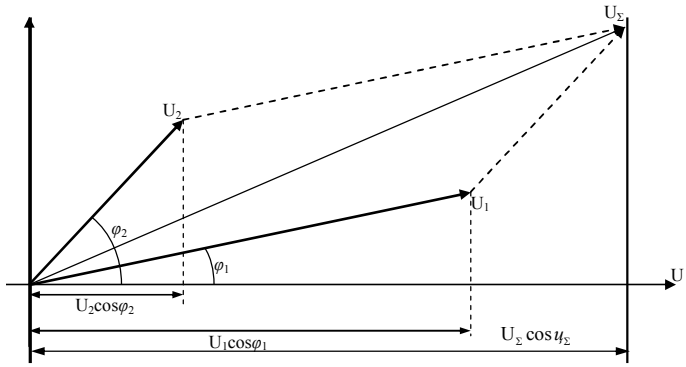

Fig. 7 Forming of reflection signal. Here: U_1, U_2 are amplitudes of reflections from 1-st and 2-nd objects, φ_1, φ_2 are corners of change of phase; $U_1 \cos\varphi_1, U_2 \cos\varphi_2$ are corresponding reflections; U_Σ it is summary amplitude and $U_\Sigma \cos\varphi_\Sigma$ is a summary signal

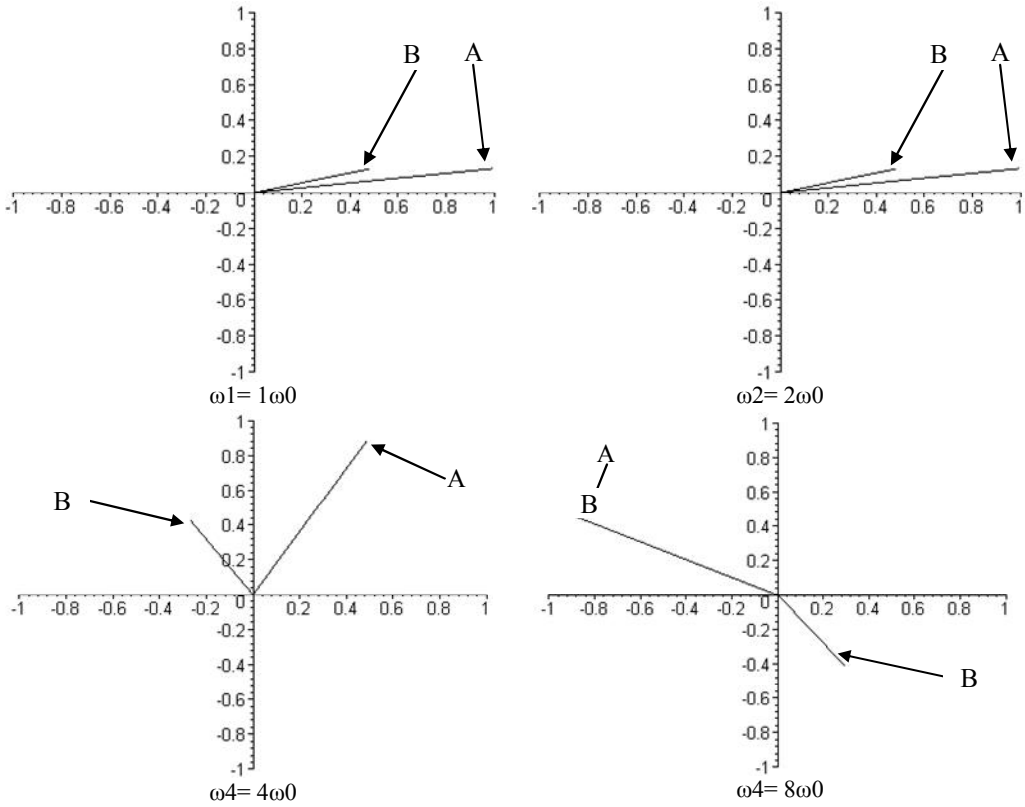

Fig. 8. To explain process of phase angle shift changes for two reflections on distances l_1, l_2 at the increases of frequency ω, ω0=4·10^3 Hz

As shown on fig. 8, at the change of test signal frequency in 2, 4 or 20 times, the angle shift changes gradually too. A change of the phase angle shift is proportional to frequency change.

Will pay attention to dynamics of change of vector A and vector B separately (table 1). Especially interesting situation for understanding processes with frequencies 12 ω and 20 ω. On these frequencies is observed transition through 2π and 4π.

Table 1. Values of phase shift angles

Frequency, ω	φ_1, *grad*	φ_2, *grad*
1 ω	19,2	38,4
2 ω	38,4	76,8
4 ω	76,8	153,6
8 ω	153,6	307,2
12 ω	230,4	460,8 (360+100,8)
20 ω	384,0 (360+24,0)	768,0 ((2x360+48)

As seen from the table 1, the increase of frequency and phase angle shift characterize every reflection. Let assume that measuring device consist of the generator of variable frequency $\omega(t_i)$. $\omega(t_i)$ is a frequency of signal during time t_i, $t_i \in [t_{i1}, t_{i2}]$. During time t_i from t_{i1} to t_{i2} frequency $\omega(t_i)$ held unchanged and duration of interval $[t_{i1}, t_{i2}]$ is enough for stabilizing of transients in a power line. As a result, we have change of phase angle shift for *i* reflection:

$$d\varphi_i = \varphi_i\left(\omega(t_2)\right) - \varphi_i\left(\omega(t_1)\right),$$

what takes place at the change of test frequency $d\omega_i = \omega(t_2) - \omega(t_1)$.

Thus will enter a term "rotation of phase angle shift" $\Omega_{i,[\omega(t_1),\omega(t_2)]}$:

$$\Omega_{i,[\omega(t_1),\omega(t_2)]} = \frac{\varphi_i\left(\omega(t_2)\right) - \varphi_i\left(\omega(t_1)\right)}{\omega(t_2) - \omega(t_1)} = \frac{d\varphi_i}{d\omega_{t_2 - t_1}}, \tag{10}$$

where t_1, t_2 are certain physical time domains at which a value of frequency of measuring signal is became.

A value of $\Omega_{i,[\omega(t_1),\omega(t_2)]}$ is a function of only frequencies and differences between the phase shift and frequencies.

In comparing with PD-FDR, value of $\Omega_{i,[\omega(t_1),\omega(t_2)]}$ is more prediction and give ability to work with low and high frequencies. It allows utilizing several intervals of frequencies in comparing with PD-FDR where wide range of frequencies required.

Let assume phase angle shift for *i*-th damage is determined from the known expression as:

$$\varphi_i = \frac{2\pi \cdot 2l_i}{\lambda},$$

or in more comfortable form circular frequency ω_j of test signal :

$$\varphi_i = \frac{2\pi \cdot 2l_i}{\upsilon} \cdot f_j = 2\frac{l_i}{\upsilon} \cdot \left(2\pi \cdot f_j\right) = 2\omega_j \frac{l_i}{\upsilon}, \tag{11}$$

where l_i – a distance to *i*-th object which a reflection is from;

υ – a speed of distribution of signal in an environment;

ω_j – a *j*-th frequency of testing signal.

In addition, expression what connect "rotation" $\Omega_{i,[\omega(t_1),\omega(t_2)]}$ of reflection vector with distance to the damage will be:

$$\Omega_i = \frac{\left(2\omega_{j+1}\frac{l_i}{\upsilon}\right) - \left(2\omega_j \frac{l_i}{\upsilon}\right)}{\omega_{j+1} - \omega_j} = 2\frac{l_i}{\upsilon} \cdot \frac{\omega_{j+1} - \omega_j}{\omega_{j+1} - \omega_j} = 2\frac{l_i}{\upsilon}. \tag{12}$$

By limitation of frequencies from $\omega_{\min}$ to $\omega_{\max}$ the turn-down of phases will lay down :

$$\varphi_{i\min} = 2\omega_{\min}\frac{l_i}{\upsilon},\ \varphi_{i\max} = 2\omega_{\max}\frac{l_i}{\upsilon}, \tag{13}$$

From (15) there is fundamental possibility not only to define frequency of reflections vectors rotation, and it is possible to define and amount of turns of vectors of phase angle shift for the *i*-th reflection in this range:

$$N_{i\,turn} = \frac{\varphi_{i\max} - \varphi_{i\min}}{2\pi}, \tag{14}$$

or

$$N_{i\,turn} = \frac{\frac{2l_i}{\upsilon}\left[\omega_{\max} - \omega_{\min}\right]}{2\pi} = \frac{\frac{2l_i}{\upsilon}\left[2\pi f_{\max} - 2\pi f_{\min}\right]}{2\pi} = \frac{2\pi\frac{2l_i}{\upsilon}\left[f_{\max} - f_{\min}\right]}{2\pi} = \frac{2l_i}{\upsilon}\left[f_{\max} - f_{\min}\right]. \tag{15}$$

The analysis of the expression (14) will give an expression for recognition (15). As a result, we receive the following: value of (15) gave to us ability to work practically with any frequency range (15). The second feature of expression (15) is that $N_{i\,циклів}$ will not be always an integer value only.

```
fL=0.5*10^-3
fR=20
fC=0.25*10^-6
fG=0.1*10^-6
fmin=0.001
fmax=600000
α[ω_]=Sqrt[1/2*((ω^2)*fL*fC-
fR*fG+Sqrt[(fR^2+(ω^2)*(fL^2))*(fG^2+(ω^2)*(fC^2))])]
```

$$\frac{\sqrt{-2.\times10^{-6} + 1.25\times10^{-10}\,\omega^2 + \sqrt{\left(1.\times10^{-14} + 6.25\times10^{-14}\,\omega^2\right)\left(400 + 2.5\times10^{-7}\,\omega^2\right)}}}{\sqrt{2}}$$

```
β[ω_]=Sqrt[1/2*(fR*fG-
(ω^2)*fL*fC+Sqrt[(fR^2+(ω^2)*(fL^2))*(fG^2+(ω^2)*(fC^2))])]
```

$$\frac{\sqrt{2.\times10^{-6} - 1.25\times10^{-10}\,\omega^2 + \sqrt{\left(1.\times10^{-14} + 6.25\times10^{-14}\,\omega^2\right)\left(400 + 2.5\times10^{-7}\,\omega^2\right)}}}{\sqrt{2}}$$

```
Z[ω_]=Sqrt[(fR+I*ω*fL)/(fG+I*ω*fC)]
```

$$\sqrt{\frac{20 + (0. + 0.0005\,i)\,\omega}{1.\times10^{-7} + (0. + 2.5\times10^{-7}\,i)\,\omega}}$$

```
γ[ω_]=β[ω]+I*α[ω]
```

$$\frac{\sqrt{2.\times10^{-6} - 1.25\times10^{-10}\,\omega^2 + \sqrt{\left(1.\times10^{-14} + 6.25\times10^{-14}\,\omega^2\right)\left(400 + 2.5\times10^{-7}\,\omega^2\right)}}}{\sqrt{2}} + \frac{i\sqrt{-2.\times10^{-6} + 1.25\times10^{-10}\,\omega^2 + \sqrt{\left(1.\times10^{-14} + 6.25\times10^{-14}\,\omega^2\right)\left(400 + 2.5\times10^{-7}\,\omega^2\right)}}}{\sqrt{2}}$$

```
Plot[α[w],{w,fmin,fmax},PlotLegends→"Expressions"]
Plot [β[w], {w, fmin , fmax }, PlotLegends  → "Expressions "]
Plot [{ Re [Z[w]], Im [Z[w]]}, {w, fmin , fmax }, PlotLegends  → "Expressions "]
```

Fig. 9. Code for modelling power line from 0,001 Hz to 600 kHz in Wolfram Mathematica

In addition, limitation of working range of frequencies is also equivalent to additional value of phase angle shift for each of signals. At $f_{\min} = 0$, an initial phase angle is always $\varphi_i \to 0$. In common case of $f_{\min} > 0$ we will also have $\varphi_i > 0$ (clearly, that except those cases, when $\varphi_i = 2\pi \cdot n$).

In real power cables, frequencies lower then 10-20 kHz does not allow to archive acceptable qualify of measuring due to variable parameters of power line on low frequencies.

For example, on fig. 9 shown code in Wolfram Mathematica for modelling power line from 0,001 Hz to 600 kHz.

After that will be received figures of phase shift $\beta[\omega]$ (fig. 10), real and imaging parts of wave impedance $\dot{Z}_{imp}[\omega]$ (fig. 11). Parameters of power line are stable for measuring only at high frequencies.

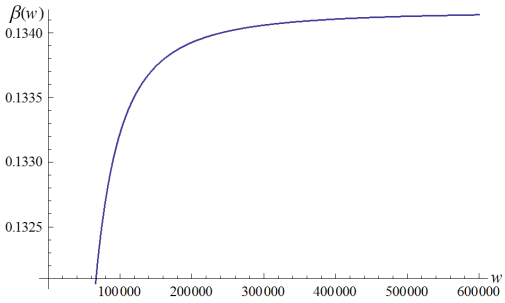

Fig. 10. Phase shift $\beta[\omega]$

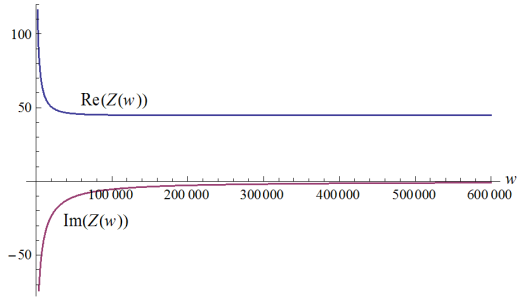

Fig. 11. real and imaging parts of wave impedance $\dot{Z}_{imp}[\omega]$.

1.5. Signal modelling

On Fig. 12 it is shown distribution of the reflected signals $0,5\cos(6\varphi)+0,7\cos(8\varphi)+0,9\cos(10\varphi)$ for the range $\varphi = 0..2\pi$. That signal for modelling power line with 3 objects in it with distance 6 : 8 : 10 respectively. As were shown on fig. 5 (a) high frequency belong to far object. Limitation in a frequency range taken from fig.10 and fig. 11. As evidently, the initial phase of signals in allowed zone are different on such condition.

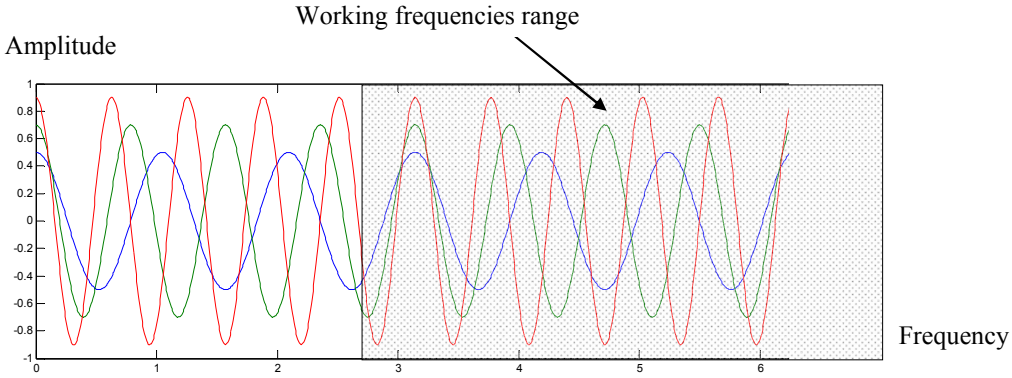

Fig. 12. Distribution of projections of vectors from the signals of reflections (signal $0,5\cos(6\varphi)+0,7\cos(8\varphi)+0,9\cos(10\varphi)$)

2. A spectral analysis of reflection signal with use of Fourier transformation with variable window size

As were specified early, signal in phase measuring methods is sum of harmonics signals of the same frequency but with different phase angle shifts (see (10)). Due to different values of φ_i values of $\Omega_{i,[\omega(t_1),\omega(t_2)]}$ are different too. So the object of analysis is a set of $\Omega_{i,[\omega(t_1),\omega(t_2)]}$.

Among the existent methods used for signal analysis, the most used methods are [1, 23, 24]:

- Fourier transformation;
- Wavelet analysis;
- Other methods of analysis.

Fourier transformation is the well-known basic instrument of signals analysis in a frequency area. It is known that the periodic signals of kind $x(t) = x(t + mT_O)$ appear as a row of a sum of harmonic constituents.

In practice of spectral analysis of the real signals does not operate a continuous signal $x(t)$ and only by the eventual sequence of their selections x(n). For this reason in the technique of digital analysis of signals, discrete Fourier transformation is used.

The one of the main problem of FFT is analysing periodical signal limited in time. There are signals with period match analysis window size. And others are not equal to analysis window. Thus, if a periodical signal does not match with FFT window size additional components appear in a spectrum. This phenomenon named spectrum leakage. Spectrum leakage is possible to illustrate with the calculation of spectrum of discrete harmonic signal (Fig. 13) on an example. Discrete signal contain a 16 points of harmonic signal with own period even to a 4 point (Fig. 13. (a) the periodically continued signal is periodic to FFT window.

If signal does not periodic to FFT window spectrum leakage will be observed (Fig. 13, (b)). Spectrum of signal consists of additional harmonics. For PD-FDR or any equivalent method this mean additional objects in line.

To determine the methods for controlling the spread of the spectrum of the input signal, it is necessary to establish the factors that lead to the occurrence of this phenomenon.

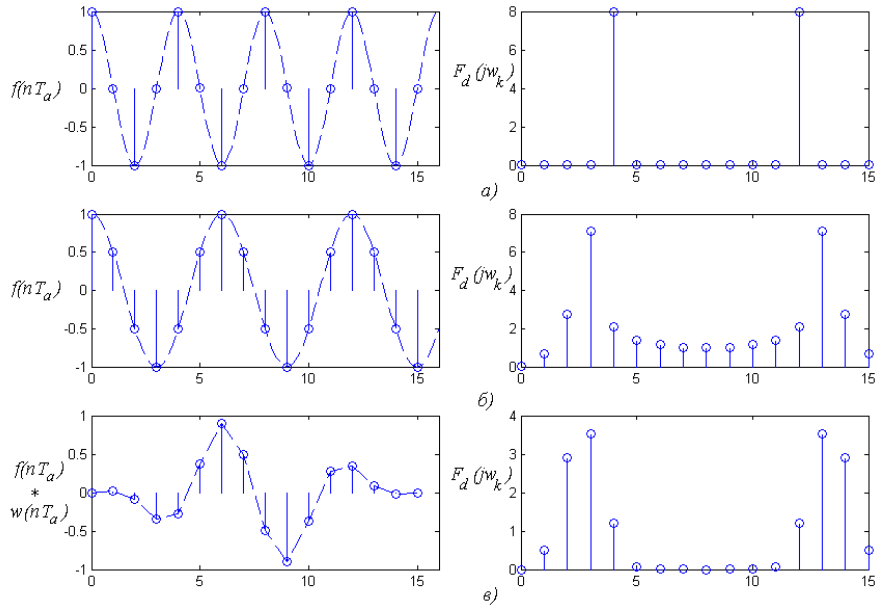

Fig. 13. FFT for periodical signal (a), unperiodical signal and spectrum leakage (b) reducing spectrum leakage with Hann window function

Understanding the causes of the phenomenon in this case will allow taking a number of measures to eliminate the spread of the spectrum.

As were shown above, the phenomenon of the spectrum leakage is the appearance of additional harmonics in the spectrum. Moreover, these additional harmonics complicate the process of identifying harmonics from the real components of the signal. That is, there is a process of "masking" the signals. In order to deal with the spectrum leakage in the practice of digital analysis, it is known that window functions are used, but in this case they do not give us the result we need because they reduce the phenomenon associated with the non-periodicity of the signal for analysis.

Window functions are used to reduce signal at beginning and ending of FFT window. For example, fig. 13 show use of Hann window function and result spectrum.

Given the complexity of the introduction of wavelet analysis and the need to create application software that would allow simple mathematical transformations, it would be able to transfer to 32-bit or 8-bit computing environment of small and medium computing power, proposed the creation of an algorithm for spectral analysis on based on the modified Fourier transform algorithm. Software implementations of the Fourier transformation are known for a large number of hardware and software environments.

2.1. A flow-chart of spectral analysis algorithm

However, existing implementations does not allow detect signals with such incomplete period, since according to the FFT, the total signal represents a series of whole-periodic functions. Thus, if we change the number of points for FFT, it is quite clear that a signal with an non integer period can transform into a signal with an integer number of periods, at the same time. But at the same time signals with integer number of periods will become signals with non integer periods.

As a result of this, it is suggested to produce multiple analyses of the same signal by FFT. However, every next time of analysis the same signal points for FFT will be reduced. Since our signal represents a sum of harmonic signals, changing the window width will be in the coincidence of the whole number of periods. Accordingly, such signals in the output of FFT will have the highest amplitudes at a certain value of the window width. Consequently, the gradual decrease in the width of the window will lead to the discovery of various spectral components in the total signal.

Since there will be a rise and fall in the spectrograph, then it is proposed to highlight the

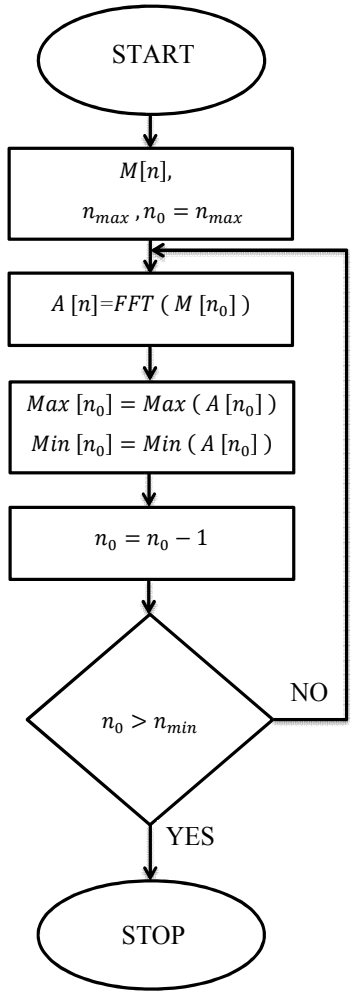

Fig. 14. Flow-chart of algorithm of spectral analysis with the change of width of window. Here $M[n]$ is an array of input data from measuring; $n_{\max}$ it is a number of the last element in an array $M[n]$; FFT it is a function of transformation of Fourier; $A[n]$ - the array of accordions is got on the i-th step of transformation; $Max[n_o]$ and $Min[n_o]$ are arrays of most and the least amplitudes of accordions.

largest and smallest values for each spectrogram in a single array. The aim of this is to determine the harmonics that have reached the highest value in the process of spectral analysis of our signal.

The algorithm for determining the spectral components of the total signal by manipulating the width of the window FFT is as follows:

1) Measuring of the input signal with the definition of N points.

2) A FFT cycle is performed. Result stored in arrays of maximal and minimal values

3) Determine the spectral components with the greatest and smallest amplitudes. The result are remembered by adding to the result to the results of the previous cycles of the FFT.

4) Reduce the width of the FFT window by dropping one point from the end.

5) If the number of readings is greater than the minimum value of N*min*, go to paragraph 2.

Conditionally, the flow-chart of algorithm of spectral analysis of signal with the change of width of window is shown on Fig. 14.

Software was created in the MatLab using the proposed algorithm.

2.2. Result of proposed algorithm

Let's consider the work of the proposed algorithm for spectral analysis of the signal with the change in the width of the FFT window. A signal is taken as a test signal (Fig. 15, a) $-20\cos(64t+0.7\pi)-32\cos(74.3t+1.2\pi)+49\cos(106.2t+3.2\pi)$.

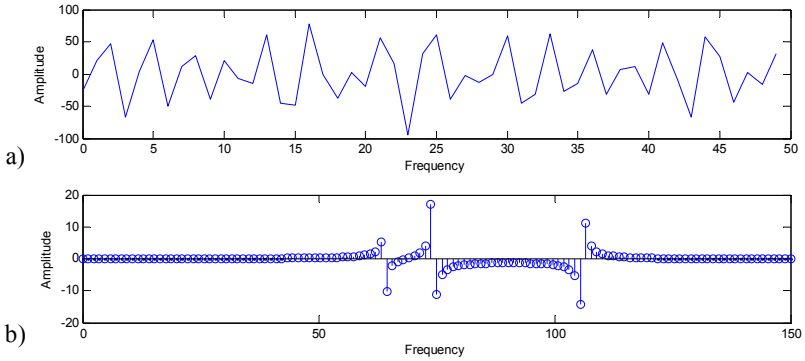

Fig. 15. Signal (a) and spectral transformation (b) for the signal of kind $S(t)=-20\cos(64t+0.7\pi)-32\cos(74.3t+1.2\pi)+49\cos(106.2t+3.2\pi)$ □

Fig. 16 shows the dynamics of changes of spectral components at the terms of FFT window width changed. It stipulates the necessity of setting of norms of the got result for a coersion to the only dimension to the landmark of frequency. At the same time, such setting of norms introduces error setting of norms, as spectral components, which have a whole number $N_{i,FFT}$ led to the corresponding rationed whole numbers:

$$N_{j,FFT}=round\left[\frac{Fs}{2}\cdot\frac{1}{NFFT'}\cdot k\right],\ k=1..NFFT',$$

$$NFFT'=NFFT/2..NFFT,$$

where Fs is frequency of input signal discretisation;

$NFFT$ it is an amount of points of FFT.

For comfort of analysis, the result after normalization is shown on Fig. 17.

After FFT as shown on fig. 15, amplitudes is only 12.1, 19.3, 16,1. After comparing result of FFT from fig. 15 and from fig. 17 can be noted following: the presence of three signals with amplitudes by modules 7.2, 13.1 and 17,4. Correlation between those amplitudes are more close to original ones in test signal.

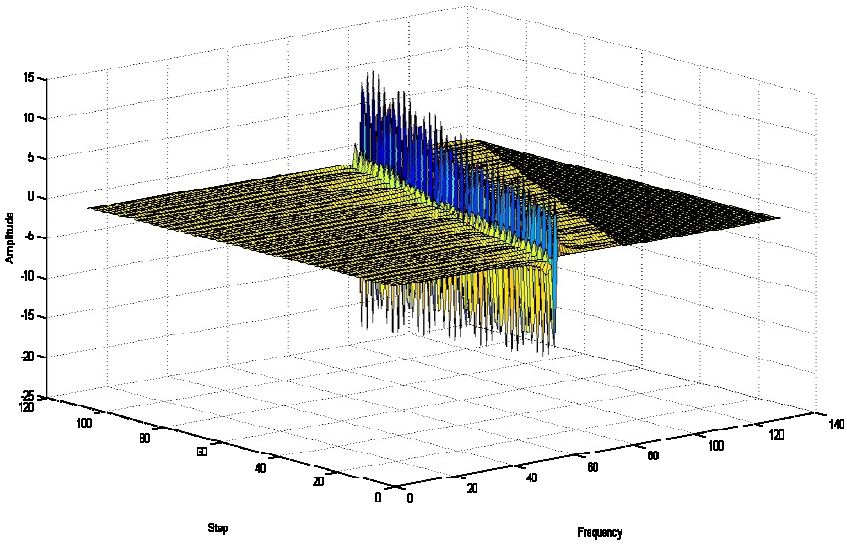

Fig. 16. Result in a 3-dimension view

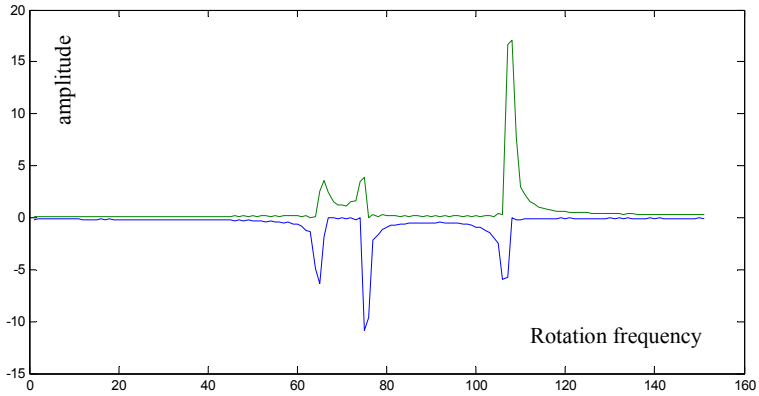

Fig. 17. Result of selection of spectral components by determination of maximal and minimum values of amplitudes of spectrums

Thus, offered method of determination of spectral component signals, which consist of harmonious signals with variables periods in compare to FFT window width allows to set both the presence of spectral components and pick up correct amplitudes of these components. After FFT as shown on fig. 15, amplitudes is only 12.1, 19.3, 16,1.

3. Conclusions

1. There are a huge number of methods of spectral analysis, but they have properties that complicate their use in practice. Fast Fourier transform is a simple analysis method. However, the Fourier transform has errors in determining the frequencies and amplitudes of the components when the width of the analysis window and the period of the input signal are not identical. Spectral analysis based on wavelet analysis is a powerful tool, but complex and not sufficiently convenient for transfer to automated measuring systems.

2. The algorithm of the spectral analysis of the signal with the change in the width of the window is proposed. A simulation has been performed. Application of a variable width of a window allows reduce the influence of the spectrum leakage.

3. It is established that existing phase measuring methods have fundamental frequency constraints, especially at low frequencies below 100 kHz. Therefore, phase measuring methods

have additional difficulties in practical application, since one of the key properties is considered to be the measurement at frequencies close to zero. At the same time, the frequency limitation is not principle for the presented phase-frequency method.

References

1. **Amara Graps**. An introduction to Wavelets. IEEE Computational Science and Engineering, Summer 1995, vol. 2, num. 2

2. **Basava, Santi B,** (2004), "Detection and location of cable faults using reflectometry methods", MS Thesis, Ulah State University.

3. Cable Testing Excerpt From Prysmian's Wire and cable engineering guide. Prysmian Cables & Systems. Revision 0. October 23, 2007. - 8 p.

4. **Chen, C, S., Rocmcr, L. E. and Grumbach, R. S.** (1978), "Cable diagnostics for power cables", IEEE Annual Conference of Electrical Eng. Problems in Rubber and Plastic Industries, 20-22, Apr.

5. **Chung, You Chung and etc.** (2003), "Non-destructive fault location on aging aircraft wiring networks Part 1-Cost-optimizcd solutions", IEEE A/'-S and USNC/URSI National Radio Science Digest, Columbus, Ohio.

6. **Chung, You Chung, Amamath, Nirmal and Furse, Cynthia,** "Capacitance and inductance sensors for open and short ends circuit wire faults detection", IEEE Trans. Instrument and Measurements, IM-8025, in review.

7. **Chung, You Chung, Turse, Cynthia, Pruitt, Jeremy,** (2005) "Application of phase detection frequency domain reflectometry for locating faults in an F-I8 flight control harness", IEEE Trans. Electromagnetic Compatibility, 47(2), 127-114.

8. **Hampton, R.N., Perkel. J., Hernandez, J.C., Begovic, M., Hans, J., Riley, R., Tyschenko, P., Doherty, F., Murray, G., Hong, L., Pearman, M.G., Fletcher, C.L., and Linte, G.C.** Experience of Withstand Testing of Cable Systems in the USA, CIGRE 2010, Paper No. B1-303

9. **Furse, C. and Kamdar, N.** (2002), "An inexpensive distance measuring system for navigation of robotic vehicle", Microwave and Optical Tech. Letters, 33(2). 84-97, April.

10. **Furse, Cynthia, Chung, You Chung, Dangol, Rakcsh, Nielsen, Marc, Mabey, Glen, Woodward, Raymond,** (2003), "Frequency domain reflectometry for on board testing of aging aircraft wiring", IEEE Trans. Electromagnetic Compatibility, 306-315, May.

11. **Hartlein R.A., Hampton R.N., Perkel J.** Some Considerations on the Selection of Optimum Location, Timing, and Technique, for Diagnostic Tests, IEEE Power Engineering Society (PES) General Meeting Panel Session, Pittsburg, PA, 2008.

12. **Oppenheim, A. V.** (1975), Digital Signal Processing, Prentice-Hall, Englewood Cliffs, N.J.

13. Overview of cable system diagnostic technologies and application : Cable Diagnostic Focus Initiative Project (CDFI) : 04-211/04-212/09-166 / The National Electric Energy Testing Research and Applications Center (NEETRAC); Hartlein, R., Hampton, N., Hernández, J.C., and Perkel, J. – Georgia, 2010. – 323 p.

14. **Schmidt, Mark** (2002), "Use of TDR for cable testing", MS Thesis, Utah State University, Logan, Utah.

15. **Smith, Paul** (2003), "Spread spectrum lime, domain reflectometry", Ph.D. dissertation, Utah Slate University.

16. **Tsai, P., Lo, C., Chung, Y. C. and Furse, C. M.** (2005), "Mixed signal reflectometer for location of faults on aging wiring", IEEE Sensor Journal, 5(6), 1479-1482.

17. **Abramov K. K.** Simulation and calculation of communication cables on the computer. Moscow. Communication, 1979. 79 p.

18. **Gillmanov Eduard Akhnafovich**. Improvement of efficiency of cable transmission lines operation on the basis of their diagnostics by pulsed reflectometry., Ufa, 2009. - 20 p.

19. **Horiaschenko K.L.** Pulse-phase measurements for a line with two inhomogeneities .Measuring and computing engineering in technological processes. Khmelnytskyi. 2003. No. 1. P. 80-82.

20. Cable products. Terms and definitions: GOST 15845-80. - Introduction. from 01.07.1981. - 18 s.

21. **Glebovich G.V., Andriyanov A.V., Vvedensky Yu.V.** Investigation of objects with picosecond pulses - Moscow: Radio and Communications, 1984. 256 pp.

22. **Lyubchik V.R.** Development of the phase method for measuring distances to two objects. Bulletin of the Technological University of Podillya. 2004. No. 2. P. 108-114.

23. **Maevsky S.M. , Bazhenov V.G., Baturevich E.K., Kuts Yu.V.** Application of methods of phase measurement for precision measurement of distances. Kiev. Higher school. 1983. 84 p.

24. **Otnes R, Enoxon L.** An applied analysis of time series: basic methods. Moscow. Mir. 1982 430 p.

Biographies

Photo	First names	Last-family name	Biography
	Kostyantyn	Horiaschenko	**Kostyantyn Horiaschenko** received PhD degree in Kyiv national university of technology and design in 2005. Khmelnitsky national university. His current research interests include control and fault diagnosis in power lines.
	Victor	Stetcuk	**Victor Stetcuk** received PhD degree in Khmelnitsky national university in 2012. Now he works at Khmelnitsky national university. His current research interests include telecommunications and power electronics.